

Bcl-x_L and UVRAG Cause a Monomer-Dimer Switch in Beclin1*

Received for publication, June 20, 2008 Published, JBC Papers in Press, July 18, 2008, DOI 10.1074/jbc.M804723200

Christian G. Noble¹, Jing-Ming Dong², Edward Manser², and Haiwei Song³

From the Institute of Molecular and Cell Biology, 61 Biopolis Dr., Proteos, Singapore 138673

Beclin1 has a key regulatory role in the initiation of autophagy and is a tumor suppressor. We have examined the interplay between viral or human Bcl-2-like proteins and UVRAG and their opposite effects on Beclin1. We show that Beclin1 forms a dimer in solution via its coiled-coil domain both *in vivo* and *in vitro*. Viral Bcl-2 binds independently to two sites on the Beclin1 dimer, one with high affinity and one with lower affinity, whereas human Bcl-x_L binds both sites equally with relatively low affinity. UVRAG disrupts the Beclin1-dimer interface, forming a heterodimer with Beclin1, suggesting that this is how UVRAG causes its effects on Beclin1 to activate autophagy. Both Bcl-2-like proteins reduce the affinity of UVRAG for Beclin1 ~4-fold, suggesting that they stabilize the Beclin1 dimer. Moreover, coimmunoprecipitation assays show that UVRAG substantially reduces Beclin1 dimerization *in vivo*. These data explain the concentration-dependent interplay between Bcl-2, UVRAG, and Beclin1, as both tumor suppressors, UVRAG and Beclin1, have single-copy mutations in human cancers. Furthermore, our data suggest that an alternative strategy for developing anti-cancer compounds would be to disrupt the Beclin1-dimer interface.

Autophagy is an intracellular vesicular pathway for the degradation of long-lived proteins and organelles (1, 2). The bulk cytoplasm is engulfed in vesicles that mature into autophagosomes and are then targeted to the lysosome. This process is well conserved from yeast to mammals, and many of the autophagy-related (*atg*) genes that are involved were originally identified in yeast (2). Many have mammalian homologues with conserved functions in autophagy. For example the mammalian protein Beclin1 is a homologue of yeast Atg6, and both form a lipid-kinase complex with class III phosphoinositide-3 kinase (PI(3)KC3⁴; Vps34 in yeast) that mediates vesicle nucleation.

Autophagy is required during cell growth and development and is thought to be predominantly a pro-survival process. For

example, it is induced in response to cellular stress such as starvation as well as during differentiation when large scale changes within cells are required. However, excessive autophagy also induces cell death by a morphologically distinct process to apoptosis, and increasing evidence suggests that autophagy can also function as a programmed-cell-death pathway that is distinct from apoptosis. For example, RNAi against *atg5*, *atg7*, or *beclin1* prevents cell death in apoptosis-incompetent mouse cells (3, 4). This suggests that cells can die by an alternative Beclin1-dependent pathway when apoptosis is inhibited.

Beclin1 is monoallelically deleted in many sporadic human breast and ovarian cancers (5), and *beclin1* gene transfer inhibits tumorigenicity, suggesting that reduced Beclin1 expression increases breast cancer progression (6). Heterozygous disruption of *beclin1* in mice increases the formation of spontaneous tumors (7, 8), showing Beclin1 is a haplo-insufficient tumor suppressor.

The Bcl-2 family of proteins regulate apoptosis (9). The Bcl-2-like proteins, including Bcl-2, Bcl-x_L, Bcl-w, Mcl-1, and A1, inhibit apoptosis, whereas the other Bcl-2 subfamilies, the Bax-like proteins, including Bax and Bak, and the Bcl-2-homology domain 3 (BH3)-only proteins are largely pro-apoptotic. Bcl-2-like proteins induce Bax and Bak to rearrange to form transmembrane pores that initiate the later stages of apoptosis, whereas BH3-only proteins bind to Bcl-2-like proteins and block their inhibition of apoptosis. Bcl-2-like proteins including Bcl-x_L and Bcl-2 bind to Beclin1 (10), and Beclin1 contains a single BH3 domain, indicating that it is also a member of the BH3-only family (10–12). Therefore, Beclin1 may sequester Bcl-2, which may be responsible for the tumor suppressor activity of Beclin1 (11). The γ -herpesviruses, such as Kaposi's sarcoma-associated herpesvirus (KSHV), encode a viral form of the cellular Bcl-2 oncogene (vBcl-2) which also bind to BH3-only proteins including Beclin1 to prevent apoptosis (13, 14).

As well as inhibiting apoptosis, Bcl-2 binding to Beclin1 also inhibits autophagy, as it blocks the lipid-kinase activity of the Beclin1-PI(3)KC3 complex and prevents vesicle initiation (14). Recently another tumor suppressor, UVRAG, has been shown to interact with Beclin1 and stimulate autophagy by activating the kinase activity of PI(3)KC3 (13). Therefore, Bcl-2 and UVRAG have opposing effects on the Beclin1-PI(3)KC3 complex. Here we have analyzed the reasons for these antagonistic effects at the molecular level by examining Beclin1 and its interacting partners. We show that the central coiled-coil domain of Beclin1 dimerizes both *in vivo* and *in vitro*. Bcl-x_L and viral Bcl-2 bind to Beclin1 by different mechanisms, but both proteins appear to stabilize the Beclin1 dimer interface, whereas

* This work was supported by the Biomedical Research Council of A*STAR (Agency for Science, Technology and Research) (to H. S.). The costs of publication of this article were defrayed in part by the payment of page charges. This article must therefore be hereby marked "advertisement" in accordance with 18 U.S.C. Section 1734 solely to indicate this fact.

¹ Present address: Novartis Institute for Tropical Diseases, 10 Biopolis Road, 05-01 Chromos, Singapore 138670.

² Supported by the GlaxoSmithKline-IMCB (GSK-IMCB) Singapore fund.

³ To whom correspondence should be addressed. Tel.: 65-65869700; Fax: 65-67791117; E-mail: haiwei@imcb.a-star.edu.sg.

⁴ The abbreviations used are: PI(3)KC3, class III phosphoinositide-3 kinase; CCD, coiled-coil domain; BH, Bcl-2 homology; ITC, isothermal titration calorimetry; KSHV, Kaposi's sarcoma-associated herpesvirus; TCEP, Tris[2-carboxyethylphosphine] hydrochloride; SBP, streptavidin-binding peptide.

UVRAG disrupts the Beclin1 dimer. Therefore, Beclin1 acts as a monomer-dimer “switch” regulated by UVRAG and Bcl-2-like proteins.

EXPERIMENTAL PROCEDURES

Protein Expression and Purification—The DNA sequences coding for Beclin1, residues 133–266 and 95–266, and KSHV Bcl-2 residues 1–146 were isolated by PCR amplification and cloned into the BamHI and XhoI restriction sites of pGEX6P-1 (Amersham Biosciences). Beclin1 residues 95–266 and KSHV Bcl-2 residues 1–146 were also cloned, respectively, into the BamHI and Sall and into the NdeI and XhoI restriction sites of pETDuet-1 (Novagen). UVRAG residues 189–275 and Beclin1 residues 133–266 were cloned, respectively, into the BamHI and Sall and into the NdeI and XhoI restriction sites of pETDuet-1. These pETDuet-1 constructs were subsequently modified to insert an N-terminal glutathione *S*-transferase fusion with a PreScission protease (Amersham Biosciences) cleavage site instead of the N-terminal His tag into the upstream gene. The double mutant variant of KSHV Bcl-2 (N67D,V117A) was created by two rounds of site-directed mutagenesis using the QuikChange site-directed mutagenesis kit (Stratagene). The individual proteins and complexes were expressed in the *Escherichia coli* strain BL21 (DE3) and purified from clarified crude cell extracts by cleaving from a glutathione affinity column using PreScission protease followed by ion-exchange and gel-filtration chromatography. Bcl-x_L (residues 1–208, N52D, N66D) in pET29b was purified as described previously (11). The nucleotide sequence of each expression clone was verified by automated DNA sequencing. Protein concentrations were determined from the absorbance at 280 nm using molar extinction coefficients derived by summing the contributions from tyrosine and tryptophan residues. The 24-mer Beclin1-BH3 peptide (residues 107–129 and an additional N-terminal tyrosine to determine the concentration by UV spectroscopy) was purchased high performance liquid chromatography-purified (1st Base).

Sedimentation Velocity—Sedimentation velocity experiments were performed using a ProteomeLab XL-A analytical ultracentrifuge (Beckman Coulter) with 2-channel centerpieces in an An-60Ti rotor at 42,000 rpm and 20 °C. Radial scans at a single wavelength (typically 280 nm) were taken every 300 s. The solvent density and viscosity and the protein partial specific volume were calculated using the program SEDNTERP. Protein samples were dialyzed into a buffer containing 20 mM Tris, pH 7.8, 150 mM NaCl, and 0.5 mM Tris[2-carboxyethylphosphine] hydrochloride (TCEP). The data were fitted to the continuous size-distribution functions $c(S)$ or $c(M)$ using the program SEDFIT (15).

Sedimentation Equilibrium—Sedimentation equilibrium experiments were performed using a ProteomeLab XL-A analytical ultracentrifuge using 6-channel centerpieces in an An-60Ti rotor at 20 °C. Protein samples were dialyzed into 20 mM Tris, pH 7.8, 150 mM NaCl, and 0.5 mM TCEP. Samples were centrifuged for ~24 h until they reached equilibrium and no further change was seen in the distribution. Radial scans were measured at 280, 250, and 230 nm. The data were fitted to an ideal single-species model as well as a rapid monomer-dimer

equilibrium using the program HETEROANALYSIS. The vBcl-2-Beclin1 BH3-CCD complex was also analyzed in terms of a heteroassociation model consisting of two sequential binding events. Where possible, scans were also taken after centrifugation at 42,000 rpm to measure the residual absorbance for initial offset values.

Isothermal Titration Calorimetry—Isothermal titration calorimetry was performed using a VP-ITC microcalorimeter (MicroCal Inc.). Samples were dialyzed into 20 mM Tris, pH 7.8, 150 mM NaCl, and 0.5 mM TCEP. The cell was loaded with 10–20 μM Beclin1 sample, and the injection syringe was loaded with 200–400 μM UVRAG-(189–275) or Bcl-2-like protein. Typically titrations consisted of 28 injections of 10 μl, with 240-s equilibration between injections. The data were analyzed using Origin 7.0.

Analytical Size-exclusion Chromatography—A superdex 200 HR 10/30 column (Amersham Biosciences) was equilibrated with 20 mM Tris, pH 7.8, 150 mM NaCl, and 0.5 mM TCEP. Protein samples in the same buffer were injected onto the column and monitored at 210 nm.

Mammalian Cell Transfection and Imaging—Full-length Beclin1, Beclin1-(95–266), Beclin1-(133–266), and full-length Bcl-x_L were cloned into pXJ-YPet. This vector consists of the YPet coding sequence (16) in place of the FLAG tag in pXJ-FLAG (17). Full-length of BCL-x_L were cloned into pXJ-YPet, pXJ-FLAG, and pXJ-mCherry vectors. UVRAG-(189–275) was cloned into pXJ-FLAG vector. Full-length Beclin1 was cloned into a vector with the streptavidin binding peptide pXJ-FLAG-SBP vector.⁵

HeLa or COS-7 cells were plated on 18 × 18-mm glass coverslips at 30% cell density. Cells were incubated with a mixture of Optifect (Invitrogen) and plasmids according to the manufacturer's protocol for 4 h and cultured in fresh medium for 2 h before fixation. MitoTracker Red CMXRos (Invitrogen) was added at 1:10,000 from a 1 mM stock to cells maintained for 30 min at 37 °C and transferred to normal medium for 30 min at 37 °C before fixation. Images were captured on an Olympus Fluoview FV1000 laser-scanning confocal microscope using a NA1.45 60× oil lens.

Streptavidin Bead Affinity Pulldown Assay and Western Blotting—COS-7 cells in 60-mm NUNC culture dishes were transfected using Lipofectamine 2000 (Invitrogen) according to the manufacturer's protocol. After 8 h fresh medium was added, and cells were cultured overnight. Total cell lysate was collected in 500 μl of lysis buffer (25 mM HEPES, pH 7.3, 100 mM NaCl, 0.15 mM MgCl₂, 0.2 mM EDTA, 5% glycerol, 1 mM dithiothreitol, 0.5% Triton X-100, 1× Complete (Roche Applied Science), 1 mM phenylmethylsulfonyl fluoride) and passed through a 26G1/2 needle (10–) before clarification (10 min at 13,000 rpm). This Triton-X-100-soluble lysate (total cell lysate, ~500 μg) was incubated with 25 μl of streptavidin-agarose (Upstate) and washed with 200 μl of phosphate-buffered saline, 0.1% Triton X-100 (3×). Bound proteins were eluted in SDS sample buffer. YPet- or FLAG-tagged proteins were detected with anti-green fluorescent protein and anti-FLAG

⁵ Z.-S. Zhao, unpublished information.

Bcl-x_L-Beclin1-UVRAG Interaction

antibodies, respectively, by Western blotting on polyvinylidene difluoride.

RESULTS

The Beclin1 CCD Forms a Dimer in Solution—Beclin1 is a tumor suppressor (6) and contains a number of structural domains, including a BH3, a coiled-coil domain (CCD), and an evolutionarily conserved domain. The evolutionarily conserved domain binds to PI(3)KC3 (18), and the CCD binds to a similar CCD of UVRAG (13), whereas the BH3 domain binds to Bcl-2 (11, 12). It has previously been shown that UVRAG binding to Beclin1 increases PI(3)KC3 kinase activity (13) and that Bcl-2 reduces this kinase activity (14). Here we have sought to understand how Bcl-2 and UVRAG cause these effects at the molecular level. First, to characterize the interactions between

Beclin1, Bcl-2, and UVRAG, we expressed the CCD of Beclin1 (residues 133–266; Beclin1 CCD) or both the BH3 and CCD domains (residues 95–266; Beclin1 BH3-CCD) in *E. coli* and purified them to near homogeneity. The final purification step involved a size-exclusion column and the Beclin1 CCD/BH3-CCD samples eluted at a much higher molecular mass than would be expected for a compact monomer or even dimer (>100 kDa; data not shown). Therefore, we further characterized both Beclin1 fragments by analytical ultracentrifugation (Fig. 1, Tables 1 and 2). Beclin1 CCD and Beclin1 BH3-CCD were both analyzed by sedimentation equilibrium over a wide concentration range. The data for both proteins fitted well to a single-species model, and both gave very similar weight-averaged molecular weights to the formula mass of a dimer showing that Beclin1 dimerizes via its CCD. No concentration dependence was seen over the concentration range used for either protein, indicating that the dimer interface is high affinity.

UVRAG CCD (residues 189–275) and KSHV Bcl-2 (excluding the transmembrane domain; hereafter referred to as vBcl-2) were also analyzed by sedimentation equilibrium. As expected, both proteins were monomeric in solution (Table 1). Bcl-x_L, lacking the transmembrane domain, has previously been shown to be monomeric (19).

The Beclin1 proteins were also analyzed by sedimentation velocity to confirm that the proteins are dimeric and to get an indication of the molecular shape (Fig. 1C, Table 2). The data were fitted using the continuous distribution functions $c(S)$ and $c(M)$. These functions fit the data to a continuous distribution of sedimentation coefficients or weight-averaged molecular weights, respectively (15). This analysis showed that both Beclin1 proteins sedimented as single species with apparent molecular weights very close to that of a dimer. Surprisingly both proteins had very high frictional ratios of ~2. Given that the

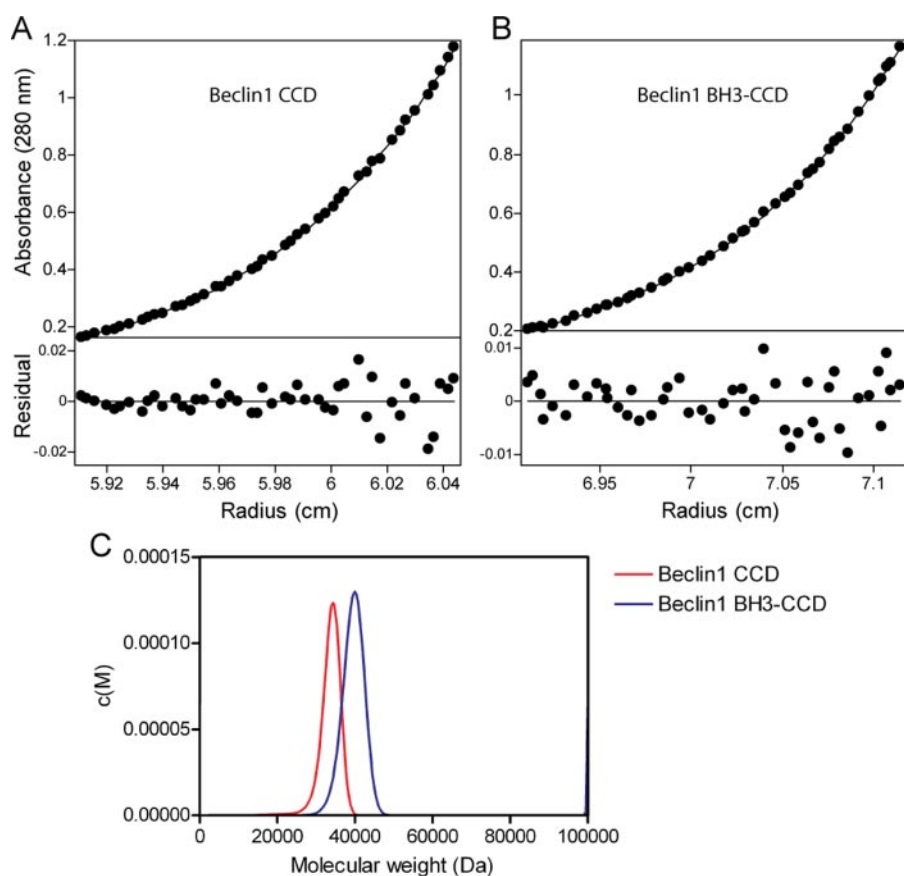


FIGURE 1. **Beclin1 CCD dimerizes in solution.** Beclin1 CCD (A) and Beclin1 BH3-CCD (B) were analyzed by sedimentation equilibrium and fitted to an ideal single-species model. Representative fits for each protein are shown. C, Beclin1 CCD and Beclin1 BH3-CCD were also analyzed by sedimentation velocity and fitted to the $c(S)$ and $c(M)$ size-distribution functions. The $c(M)$ distribution is shown for both proteins.

TABLE 1

Summary of sedimentation equilibrium data

Protein	Partial specific volume	M_r	Fitted M_r	Concentration range		Rotor speeds	Stoichiometry	K_a
				μM	krpm			
Beclin1 CCD	0.7211	16,660	32,430	3–165	20, 23, 26	Dimer		
Beclin1 BH3-CCD	0.7213	20,720	41,810	2–145	16, 18, 20	Dimer		
UVRAG	0.7507	10,490	11,510	2–20	30, 32, 34	Monomer		
vBcl-2	0.7431	16,620	17,370	1–22	20, 23, 26	Monomer		
Beclin1 BH3-CCD + vBcl-2	0.7213, 0.7431	41,440, 16,200		0.3–15	14, 16, 18	2:2	5.55×10^7 1.13×10^6	
Beclin1 BH3-CCD + Bcl-x _L	0.7199	41,440, 24,290	65,070	0.5–17	14, 17, 20	2:2		
Beclin1 CCD + UVRAG CCD	0.7326	10,490, 16,660	30,010	13–74	18, 21, 24	1:1		

Beclin1 CCD is largely α -helical in solution (13), this shows that both proteins are highly asymmetric.

vBcl-2 Binds to Two Distinct Sites on the Beclin1 Dimer—To test whether Beclin1 remains dimeric on binding to Bcl-2-family proteins, we analyzed the binding of vBcl-2 and Bcl-x_L to the Beclin1

TABLE 2
Summary of sedimentation velocity data

Protein	S_{app} (from $c(S)$)	$S_{20,w}$	f/f_0	M_r	M_r (from $c(M)$)
Beclin1 CCD	1.95	2.02	1.96	16660	34200
Beclin1 BH3-CCD	2.09	2.17	2.01	20720	40000
Beclin1 BH3-CCD vBcl-2	3.24	3.36	1.63	73840	58800
Beclin1 BH3-CCD Bcl-x _L	3.14	3.26	1.86	89990	64600

BH3-CCD dimer by isothermal titration calorimetry (ITC). These Bcl-2 proteins were used because of their high solubility and because both human Bcl-x_L and vBcl-2 bind to Beclin1 and inhibit autophagy (14). Double mutant variants of both Bcl-2-like proteins were used because this increases their solubility (11, 20). The titration curve for vBcl-2 clearly shows biphasic binding, and therefore, the data were fitted to a two-site binding model (Fig. 2A, Table 3). One high affinity interaction occurred at a molar ratio of ~ 0.5 , *i.e.* 1 vBcl-2 per Beclin1 dimer, and the second interaction occurred at a molar ratio of ~ 1 , *i.e.* 2 vBcl-2 per Beclin1 dimer. Therefore, these data show that the Beclin1 dimer contains two distinct vBcl-2 binding sites, one with high affinity and one with lower affinity. The equilibrium dissociation constant (K_d) for the higher affinity site is 25 nM, whereas for the lower affinity site it is 4.8 μ M.

To confirm the existence of higher and lower affinity Bcl-2-binding sites, we co-expressed and purified a complex of vBcl-2 and Beclin1 BH3-CCD and analyzed it by sedimentation velocity and sedimentation equilibrium (Fig. 2B, Tables 1 and 2). The sedimentation equilibrium data were analyzed in terms of heteroassociation models with either a single vBcl-2 or two distinct vBcl-2 molecules binding to the Beclin1 dimer. The data could not be fitted to a single-association model but fitted very well to a model incorporating two separate binding events, and the dissociation constants were similar to those seen with the ITC data. Therefore, this confirms that Beclin1 binds two Bcl-2 molecules, one with high affinity and one with lower affinity.

To examine whether the high affinity Bcl-2-binding site on Beclin1 is created by dimerization of Beclin1, we measured binding between vBcl-2 and a Beclin1-BH3 peptide residues 107–129, which has been shown to be bound tightly in a hydrophobic groove created by helices $\alpha 2$ – $\alpha 5$ of Beclin1 (11) (Fig. 2C). The data fitted to a single binding-site model with a very similar affinity to that seen for the lower affinity binding site on the Beclin1 dimer (K_d 5.6 μ M). Therefore, dimerization is required to form the higher affinity vBcl-2 binding site on Beclin1.

Bcl-x_L Binds to Beclin1 by a Different Mechanism—Bcl-x_L bound very differently to Beclin1, and only a single binding event was detected

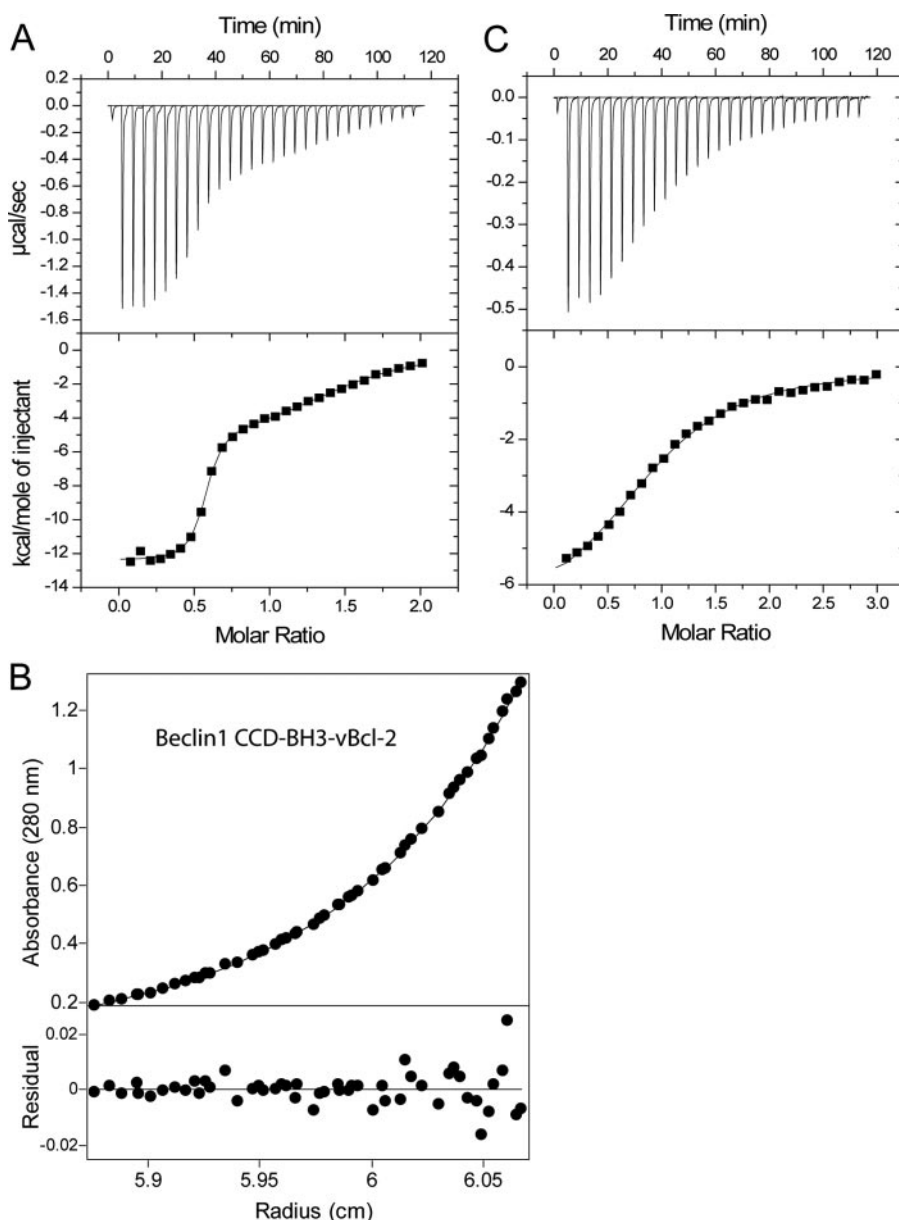


FIGURE 2. Two vBcl-2 molecules bind the Beclin1 dimer; one with high and one lower affinity. A, binding isotherm using ITC for vBcl-2 in the injection syringe titrated into Beclin1 BH3-CCD in the cell. The data were fitted to a two-site binding model (*lower panel*). B, a complex of vBcl-2-Beclin1 BH3-CCD was co-purified and analyzed by sedimentation equilibrium. The data were fitted to a heterodimer model in which vBcl-2 bound by two separate events to the Beclin1 dimer. A representative fit is shown. C, ITC titration for vBcl-2 in the syringe and Beclin1 BH3 peptide in the cell, and the data were fitted to a single-site model.

Bcl-x_L-Beclin1-UVRAG Interaction

TABLE 3

Summary of isothermal titration calorimetry data

Cell ligand	Injectant	<i>n</i>	<i>K_d</i> <i>M</i> ⁻¹	ΔH <i>Kcal · mol</i> ⁻¹	<i>T</i> ΔS (293K) <i>Kcal · mol</i> ⁻¹
Beclin1 BH3-CCD	vBcl-2	0.545 ± 0.004	4.02 × 10 ⁷ ± 6.8 × 10 ⁶	-1.242 × 10 ⁴ ± 68	-7.56
		0.929 ± 0.02	2.08 × 10 ⁵ ± 3.5 × 10 ⁴	-5.36 × 10 ³ ± 276	6.04
Beclin1 BH3 peptide	vBcl-2	0.964 ± 0.02	1.77 × 10 ⁵ ± 1.0 × 10 ⁴	-7.10 × 10 ³ ± 161	-0.20
Beclin1 BH3-CCD	Bcl-x _L	0.978 ± 0.004	9.08 × 10 ⁵ ± 4.6 × 10 ⁴	-1.09 × 10 ⁴ ± 63	-9.82
Beclin1 BH3 peptide	Bcl-x _L	0.952 ± 0.002	1.54 × 10 ⁶ ± 3.0 × 10 ⁴	-1.32 × 10 ⁴ ± 29	-16.6
Beclin1 BH3-CCD	UVRAG CCD	1.02 ± 0.01	2.04 × 10 ⁵ ± 1.2 × 10 ⁴	1.12 × 10 ⁴ ± 240	62.4
Beclin1 BH3-CCD (2× UVRAG CCD)	vBcl-2	0.976 ± 0.017	4.59 × 10 ⁵ ± 5.6 × 10 ⁴	-500 ± 118	8.83
Beclin1 BH3-CCD (2× UVRAG CCD)	Bcl-x _L	0.954 ± 0.002	1.16 × 10 ⁶ ± 2.2 × 10 ⁴	-1.14 × 10 ⁴ ± 32	-11.0
Beclin1 BH3-CCD (2× vBcl-2)	UVRAG CCD	1.06 ± 0.06	4.99 × 10 ⁴ ± 8.4 × 10 ³	1.58 × 10 ⁴ ± 1680	75.5
Beclin1 BH3-CCD (0.5× vBcl-2)	UVRAG CCD	1.02 ± 0.02	1.85 × 10 ⁵ ± 1.2 × 10 ⁴	1.24 × 10 ⁴ ± 312	66.3
Beclin1 BH3-CCD (2× Bcl-x _L)	UVRAG CCD	1.0	4.66 × 10 ⁴ ± 1.8 × 10 ³	5.53 × 10 ⁴ ± 1254	210

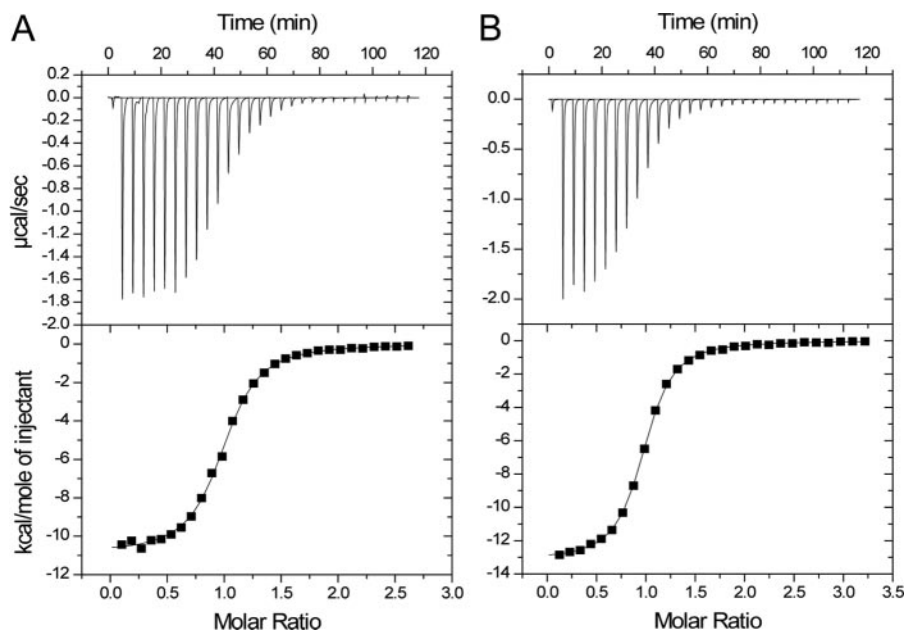


FIGURE 3. Bcl-x_L binds to Beclin1 by a different mechanism from vBcl-2. ITC titrations with Bcl-x_L in the syringe and Beclin1 BH3-CCD (A) or Beclin1 BH3 (B) peptide in the cell. The data were fitted to single-site models.

by ITC (Fig. 3), with a *K_d* of 1.1 μM. Therefore, Bcl-x_L binds to each BH3 domain of the Beclin1 dimer with a similar affinity. To rule out the possibility that Bcl-x_L binds to monomeric Beclin1, a complex of Beclin1 and Bcl-x_L was purified by gel filtration and analyzed by sedimentation equilibrium and sedimentation velocity (Tables 1 and 2). The equilibrium data globally fitted to a weight-averaged molecular mass of 65 kDa, and individual scans showed a concentration dependence and fitted to between 58 and 68 kDa. This is considerably greater than that for a Bcl-x_L-Beclin1 heterodimer (*M_r* 45) showing that Beclin1 BH3-CCD remains dimeric and is capable of binding two Bcl-x_L molecules. The velocity data were analyzed by the *c*(*M*) method, and the major species gave a similar molecular mass of ~64 kDa.

Binding between Bcl-x_L and the Beclin1-BH3 peptide was also measured to examine the effect of Beclin1 dimerization on the Beclin1-Bcl-x_L interaction (Fig. 3B, Table 3). Bcl-x_L actually bound to the peptide with a higher affinity than to the Beclin1 dimer (*K_d* 0.65 versus 1.1 μM). This result shows that dimerization of Beclin1 is not required for Bcl-x_L binding and suggests

that Bcl-x_L makes additional unfavorable interactions on binding to the Beclin1 dimer.

UVRAG Binds to Beclin1 and Disrupts the Dimer Interface—The interaction between Beclin1 BH3-CCD and UVRAG CCD was also characterized by ITC (Fig. 4A). The titration curve for this interaction was fitted to a single-site model, and binding occurred at a molar ratio of 1, showing that Beclin1 and UVRAG bind with a 1:1 stoichiometry (*K_d* 4.9 μM). This interaction was highly endothermic and, therefore, was driven entirely by entropy at 20 °C (*T* ΔS , 62 kcal·mol⁻¹; Table 3). One possible explanation for this entropy-driven binding is that UVRAG disrupts an ordered Beclin1-dimer interface. To test this possibility we analyzed Beclin1 CCD, UVRAG CCD, and a mixture of the two by size-exclusion chromatography (Fig. 4B). A peak corresponding to a lower molecular weight than the Beclin1 CCD dimer is seen when the two proteins are mixed that is not present when either is analyzed alone, indicating that the two proteins form a complex of an intermediate molecular weight.

Only a small amount of the complex was detected, presumably due to the low affinity of the interaction and the fact that both proteins have very different shapes (data not shown). Nevertheless this result was reproducible and also occurred for Beclin1 BH3-CCD mixed with UVRAG. To confirm this finding, we also analyzed an equimolar mixture of Beclin1 CCD and UVRAG CCD by sedimentation equilibrium (Table 1). All the individual equilibria fitted to mass-averaged molecular masses of 26–33 kDa and globally fitted to 30 kDa, less than the Beclin1-dimer molecular mass of 33 kDa. Given that the molecular mass of 2:1 or 2:2 Beclin1·UVRAG complexes would be 44 or 54 kDa, respectively, this shows that the sample consists of an equilibrium between a Beclin1 homodimer and a Beclin1-UVRAG heterodimer, suggesting that UVRAG may disrupt the Beclin1-dimer interface.

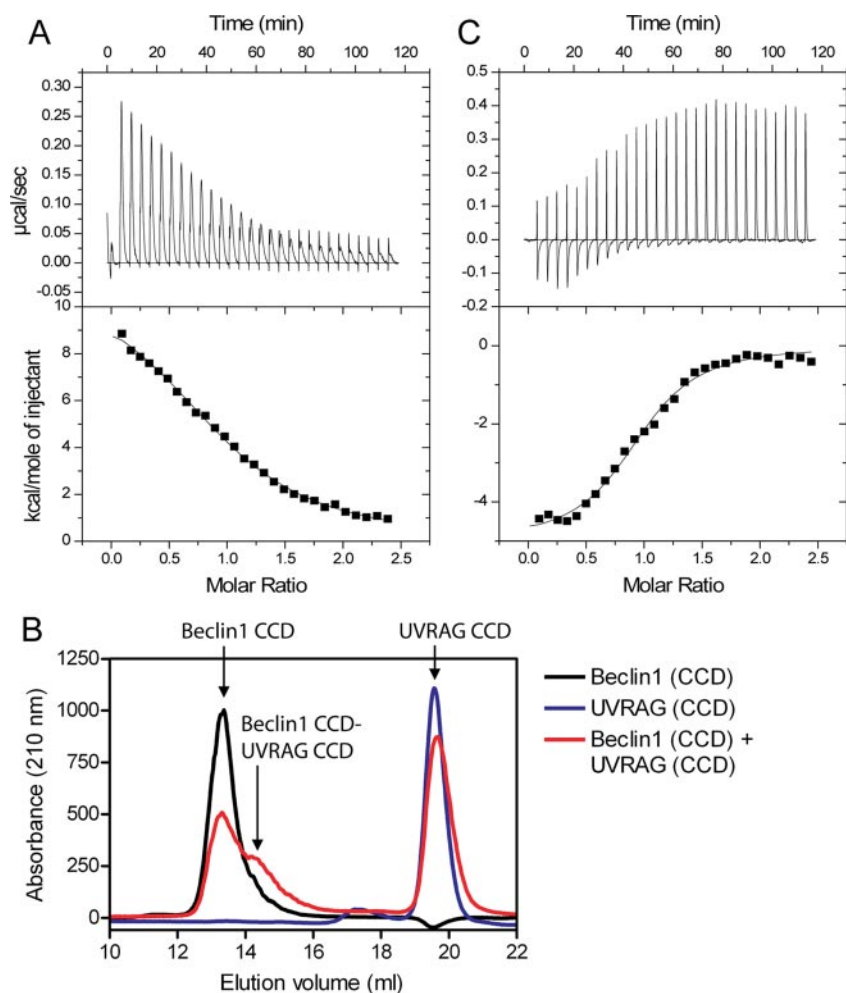


FIGURE 4. **UVRAG disrupts the Beclin1 dimer interface.** A, ITC titration for UVRAG CCD in the injection syringe and Beclin1 BH3-CCD in the cell. B, analytical gel-filtration profiles, measured at 210 nm for Beclin1 CCD, UVRAG CCD, or a mixture of the two. C, ITC titration for vBcl-2 in the injection syringe and Beclin1 BH3-CCD in the cell in the presence of a 2-fold excess of UVRAG CCD. The ITC data were fitted to a single-site model.

To further confirm that UVRAG really disrupts the Beclin1-dimer interface, binding between vBcl-2 and Beclin1 BH3-CCD was measured in the presence of a 2-fold molar excess of UVRAG (Fig. 4C). If UVRAG disrupts the Beclin1 dimer interface, one would expect that the high affinity interaction between vBcl-2 and Beclin1 would be removed. This binding isotherm was substantially different from that seen in the absence of UVRAG (compare Fig. 2A with Fig. 4C), and a single binding event occurred at a molar ratio of 1 showing that UVRAG does indeed bind a Beclin1 monomer. The interaction fitted to a K_d of 2.2 μM , *i.e.* much more similar to the lower affinity site seen in Fig. 2A. A similar experiment performed for Bcl-x_L binding to Beclin1 BH3-CCD in the presence of a 2-fold excess of UVRAG CCD (Table 3) showed that UVRAG had little effect on the interaction between Bcl-x_L and Beclin1 BH3-CCD.

Bcl-2-like Proteins Reduce the Affinity of UVRAG for Beclin1—To examine the effect of the Bcl-2-like proteins on the UVRAG-Beclin1 interaction, we performed further ITC titrations between UVRAG and Beclin1 BH3-CCD in the presence of a 2-fold molar excess of vBcl-2 or Bcl-x_L (Fig. 5; Table 3). The titrations both show that UVRAG still binds to Beclin1 but with a reduced affinity. The K_d is reduced from 4.9 to $\sim 20 \mu\text{M}$ in both cases. Therefore, both vBcl-2 and Bcl-x_L reduce the affinity of UVRAG for Beclin1 to a similar extent.

The entropy driving both interactions is increased with respect to the Beclin1-UVRAG interaction alone, consistent with UVRAG breaking additional interactions on binding to the Bcl-2-x_L-Beclin1 complex. This is particularly apparent for UVRAG binding to the Bcl-x_L-Beclin1 complex ($T\Delta S$, 210 kcal·mol⁻¹). It is not clear why vBcl-2 and Bcl-x_L affect the affinity of UVRAG for Beclin1 by the same amount given the different manner of vBcl-2 and Bcl-x_L binding to Beclin1. Therefore, we tested

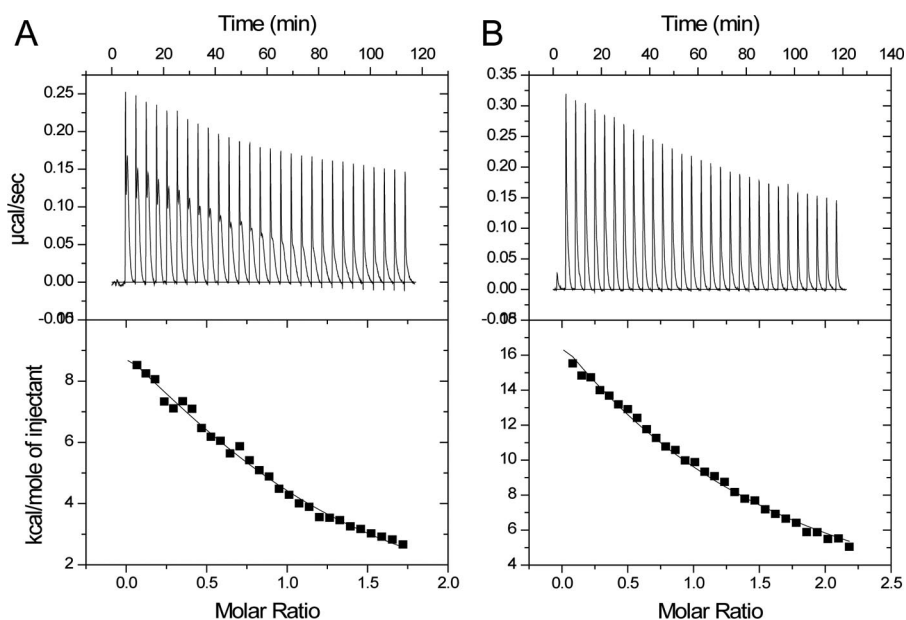


FIGURE 5. **Bcl-x_L and Bcl-2 have a similar effect on the affinity of UVRAG for Beclin1.** ITC titrations for UVRAG CCD in the syringe and Beclin1 BH3-CCD in the cell in the presence of a 2-fold excess of vBcl-2 (A) or Bcl-x_L (B). The data were fitted to a single-site model and in the presence of Bcl-x_L, *n* was held constant at 1.

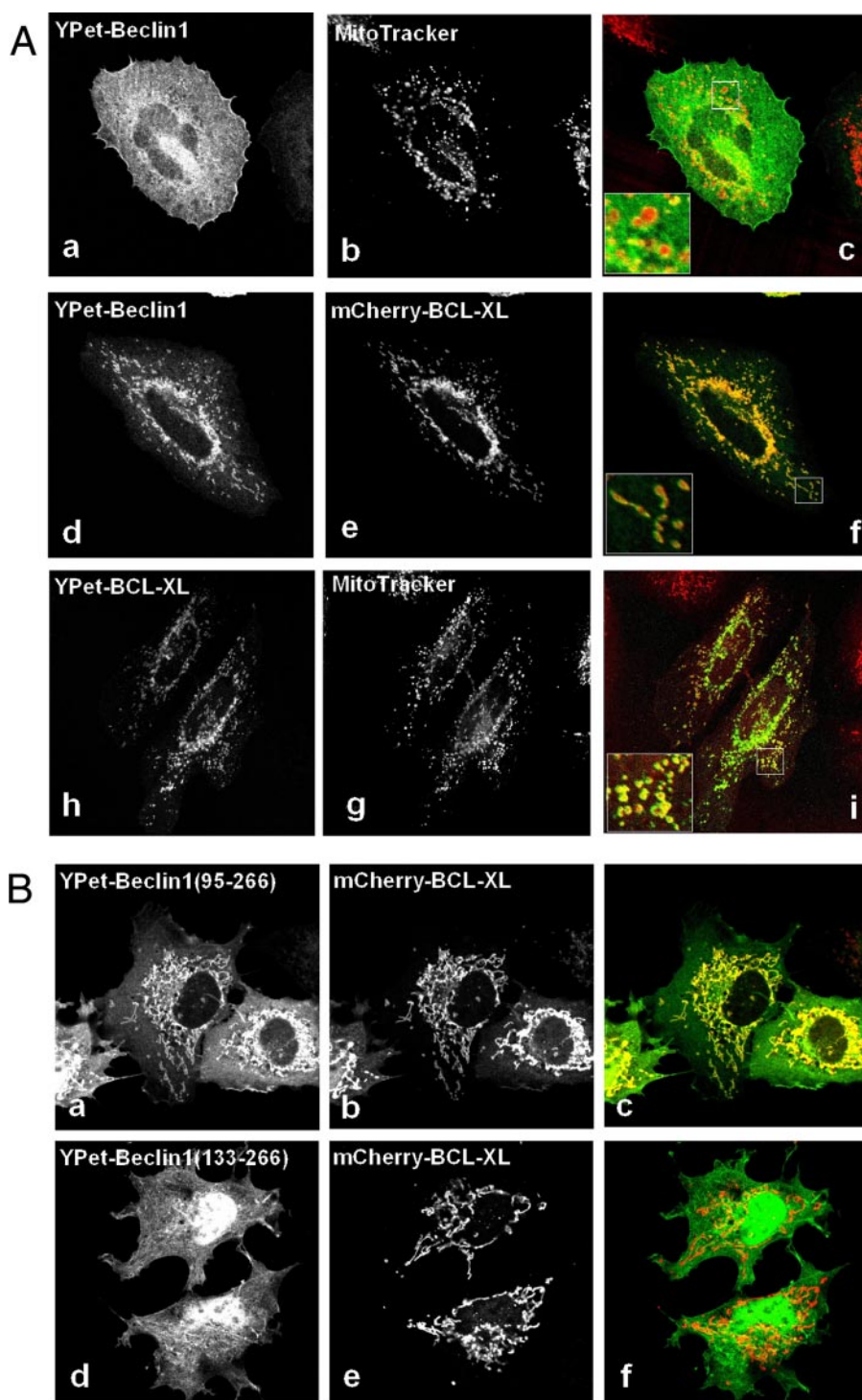


FIGURE 6. Beclin1 co-localization with Bcl-x_L in mitochondria is dependent on its BH3 domain. *A*, HeLa cells were transfected with YPet-Beclin1 (*a–c*), YPet-Beclin1 and mCherry-Bcl-x_L (*d–f*), or YPet-Bcl-x_L (*h–i*) and fixed after 6 h. Mitochondrial co-localization was assessed using MitoTracker (*b* and *g*). *Panels c, f, and i* are merged images of *a* and *b*, *d* and *e*, and *g* and *h*, respectively. The *insets* show an enlarged area (×3.4). *B*, representative images of COS-7 cells expressing YPet-Beclin1(95–266) and mCherry-Bcl-x_L (*a–c*) or YPet-Beclin1(133–266) and mCherry-Bcl-x_L (*d–f*). *Panels c and f* are merged images of *a* and *b* and/or *d* and *e*, respectively.

whether occupation of the high affinity site on Beclin1 alone could affect the affinity of the UVRAG-Beclin1 interaction. To do this we measured binding between UVRAG CCD and Beclin1 BH3-CCD in the presence of a 0.5 molar ratio of vBcl-2 (*i.e.* 1 vBcl-2 per Beclin1 dimer), but the affinity and energetics

of the UVRAG-Beclin1 interaction were unaffected (Table 3). This indicates that both vBcl-2 molecules need to be bound to reduce the affinity of UVRAG for Beclin1.

Beclin1 Co-localizes with Bcl-x_L in the Mitochondria and Dimerizes via Its CCD Domain in Vivo—To determine whether Beclin1 binds to Bcl-x_L *in vivo*, we expressed full-length Beclin1 as a fusion with YPet in HeLa cells. Beclin1 localized mainly to the cytoplasm with no obvious specific subcellular features (Fig. 6*A, a–c* (21)). When Beclin1 was co-expressed with Bcl-x_L, then both proteins were predominantly co-localized at the mitochondria (Fig. 6*A, d–f*) agreeing with previous data showing that Beclin1 interacts with Bcl-x_L *in vivo* (12, 14). Localization to the mitochondria was confirmed by fluorescent MitoTracker staining of HeLa cells expressing Bcl-x_L. Beclin1 BH3-CCD co-localized with Bcl-x_L, but Beclin1 CCD, which lacks the BH3 domain, did not (Fig. 6*B*), showing that the Beclin1 interaction with Bcl-x_L is dependent on the BH3 domain *in vivo*.

To show that Beclin1 homodimerizes *in vivo* via its CCD domain, we performed streptavidin pulldown experiments, with FLAG-SBP-Beclin1, which contains a streptavidin-binding peptide (SBP, Fig. 7*A*). YPet-Beclin1, YPet-Beclin1 BH3-CCD, YPet-Beclin1 CCD, and YPet-Bcl-x_L all interacted with FLAG-SBP-Beclin1, showing that Beclin1 dimerizes *in vivo* via its CCD domain. YPet alone did not interact with FLAG-SBP-Beclin1, showing that the interaction is specific.

UVRAG Reduces Dimerization of Beclin1—To examine the effects of UVRAG and Bcl-x_L on the homodimerization of Beclin1 *in vivo*, Beclin1 BH3-CCD (residues 95–266) and UVRAG CCD (residues 189–275) were used since the co-expressed full-length proteins were essentially Triton X-100-insoluble (data not shown). Beclin1 dimerization was assessed by the ability of the SBP-Beclin1 to bring down YPet-Beclin1. As shown in Fig. 7*B*, the dimerization of Beclin1 was unaffected by co-transfection of Bcl-x_L but reduced significantly by

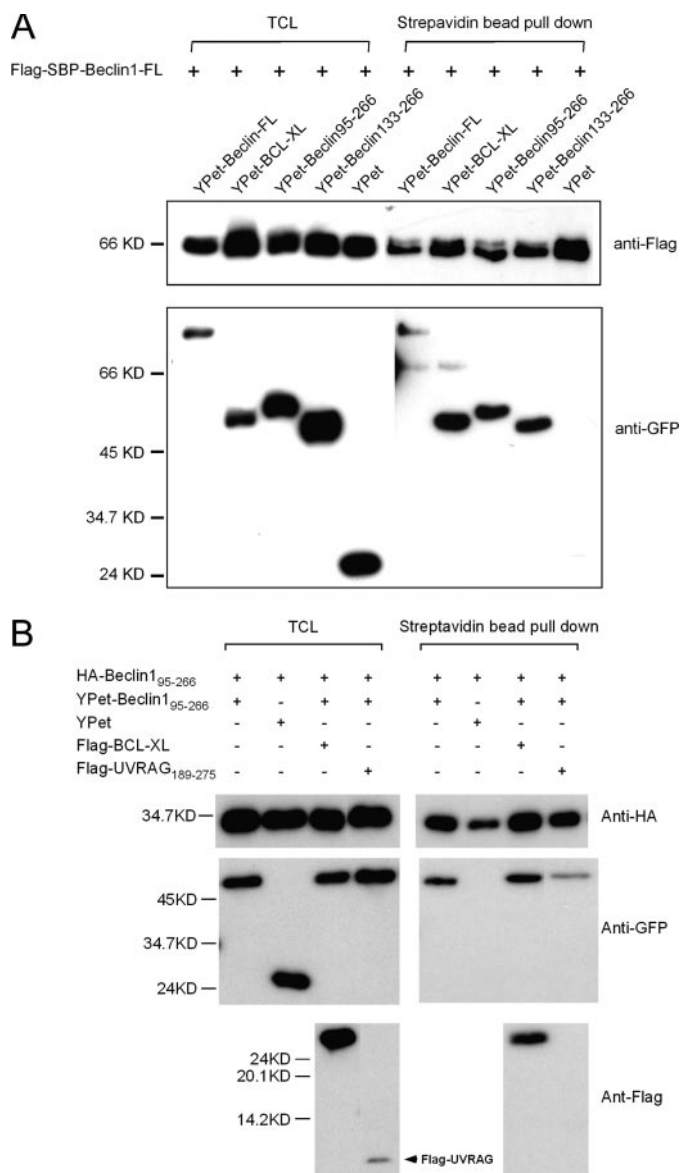


FIGURE 7. Beclin1 dimerizes via its CCD domain and this interaction is inhibited by UVRAG *in vivo*. A, COS7 total cell lysate (TCL, 400 μ g) co-expressing FLAG-SBP-Beclin1 and YPet-fusion proteins as indicated were collected on 25 μ l of streptavidin-agarose beads, and after washing, 10% of material was assessed by Western blotting for bound YPet proteins. Total cell lysate (5%) was used for comparison. GFP, green fluorescent protein. B, COS7 cells expressing hemagglutinin (HA)-Beclin1 BH3-CCD, YPet-Beclin1 BH3-CCD, and FLAG constructs as indicated were collected on 25 μ l of streptavidin-agarose beads and processed as for A.

UVRAG CCD co-expression. These results support the *in vitro* biophysical data, and together they provide strong evidence that UVRAG blocks Beclin1 dimerization.

DISCUSSION

It has previously been shown that UVRAG and Bcl-2-like proteins have antagonistic effects on the activation of autophagy. UVRAG binds to the CCD of Beclin1 and activates PI(3)KC3 leading to the initiation of autophagy (13), whereas Bcl-2-like proteins inhibit Beclin1-dependent activation of PI(3)KC3 activity and autophagy (14). In this work we have identified how these effects are conferred through Beclin1 by characterizing Beclin1 and its interactions with UVRAG and

Bcl-2-like proteins *in vitro* and *in vivo*. Our data show that Beclin1 forms a high affinity dimer and that this dimerization can be regulated by the Bcl-2-like proteins Bcl-x_L and vBcl-2 or by UVRAG. UVRAG disrupts the Beclin1-dimer, forming a heterodimer with Beclin1. Because UVRAG binding to Beclin1 activates PI(3)KC3 activity (13), it is very likely that monomerization of Beclin1 activates the kinase, possibly by allowing the kinase to bind to Beclin1. The Beclin1 dimer appears to be stabilized by the Bcl-2-like proteins, presumably by protein-protein interactions, but the molecular mechanism of this stabilization remains elusive. One possibility is that Bcl-x_L forms a transient domain-swapped dimer on binding to Beclin1, thereby stabilizing the Beclin1 dimer. A domain-swapped dimer of Bcl-x_L involving swapping of α -helix 1 at the N terminus has been observed in the recent crystal structure of Bcl-x_L bound to the BH3 domain of Beclin1 (11), but such a domain-swapped dimer has not been shown to occur in solution (11, 24). It may occur transiently when bound to dimeric BH3-only proteins, with a relatively low activation barrier such that its formation is reversible.

Bcl-x_L has also been shown to form a different domain-swapped dimer in solution, involving swapping the C-terminal α -helices 7 and 8 (22, 23). Bcl-x_L is predominantly monomeric *in vitro*, and dimerization is promoted by heat and alkaline pH. The function of this dimer formation remains unclear, and dimers and higher order oligomers have been suggested to mediate pore formation in membranes during apoptosis (23). The energy barrier for forming the C-terminal domain-swapped dimer is relatively high, and dimerization is inhibited by the BH3 domain from BID (22). Therefore, it seems unlikely that this form of swapping occurs when bound to the Beclin1 dimer.

The effects of Bcl-x_L and UVRAG on Beclin1 are modest, probably so that the reaction is reversible. For example the equilibrium dissociation constant for the interaction between UVRAG and Beclin1 is increased from \sim 5 to \sim 20 μ M in the presence of Bcl-x_L. This indicates that the change in Beclin1 monomer/dimerization is likely to be very sensitive to the local concentrations of Bcl-2-like proteins and UVRAG, as neither prevents the other from binding. An increase in UVRAG will push the equilibrium toward Beclin1 monomers, increasing the kinase activity and autophagy, whereas an increase in the Bcl-2-like protein pushes the equilibrium toward Beclin1 dimer and inhibition of autophagy. Therefore, we suggest that Beclin1 acts as a monomer-dimer switch to control autophagy. This would explain why both UVRAG and Beclin1 are haplo-insufficient tumor suppressors, *i.e.* loss of a single allele of each is found in human cancers (5, 7, 8, 25). Further research will be required to identify how this Beclin1 switch transmits its effects to PI(3)KC3. The PI(3)KC3 binding site on Beclin1 includes the CCD domain of Beclin1 as well as the evolutionarily conserved domain (13). It may be that Beclin1 must be monomeric for PI(3)KC3 to stably interact with the CCD domain and form an active complex to initiate autophagy.

It is not clear whether this concentration-dependent switch mechanism is used by other BH3 proteins to regulate apoptosis, as there is little indication of other BH3-only proteins forming homodimers. However, a single-allele knock-out of another BH3

Bcl-x_L-Beclin1-UVRAG Interaction

protein, Bim, is counteracted by a Bcl-2 deficiency (26), showing that the relative levels of Bcl-2-like and BH3-only proteins is crucial in deciding whether programmed cell death occurs.

The interplay between Bcl-2-like proteins and UVRAG also suggests novel approaches for the development of anti-cancer agents. An important consequence of this mechanism is that compounds that disrupt the Beclin1-dimer interface or stabilize the interaction with UVRAG would be expected to activate autophagy and autophagic cell death. It will be important in future research to demonstrate that monomerization of Beclin1 alone can activate autophagy and autophagic cell death and thereby demonstrate that this is a *bona fide* anti-cancer target.

Acknowledgments—We thank Yigong Shi and Adam Oberstein for providing the Bclx_L construct, and Peter Erb and Isabelle Widmer for the gift of KSHV Bcl-2 cDNA.

REFERENCES

1. Levine, B., and Yuan, J. (2005) *J. Clin. Investig.* **115**, 2679–2688
2. Levine, B., and Klionsky, D. J. (2004) *Dev. Cell* **6**, 463–477
3. Shimizu, S., Kanaseki, T., Mizushima, N., Mizuta, T., Arakawa-Kobayashi, S., Thompson, C. B., and Tsujimoto, Y. (2004) *Nat. Cell Biol.* **6**, 1221–1228
4. Yu, L., Alva, A., Su, H., Dutt, P., Freundt, E., Welsh, S., Baehrecke, E. H., and Lenardo, M. J. (2004) *Science* **304**, 1500–1502
5. Aita, V. M., Liang, X. H., Murty, V. V., Pincus, D. L., Yu, W., Cayanis, E., Kalachikov, S., Gilliam, T. C., and Levine, B. (1999) *Genomics* **59**, 59–65
6. Liang, X. H., Jackson, S., Seaman, M., Brown, K., Kempkes, B., Hibshoosh, H., and Levine, B. (1999) *Nature* **402**, 672–676
7. Yue, Z., Jin, S., Yang, C., Levine, A. J., and Heintz, N. (2003) *Proc. Natl. Acad. Sci. U. S. A.* **100**, 15077–15082
8. Qu, X., Yu, J., Bhagat, G., Furuya, N., Hibshoosh, H., Troxel, A., Rosen, J., Eskelinen, E. L., Mizushima, N., Ohsumi, Y., Cattoretti, G., and Levine, B. (2003) *J. Clin. Investig.* **112**, 1809–1820
9. Cory, S., and Adams, J. M. (2002) *Nat. Rev. Cancer* **2**, 647–656
10. Liang, X. H., Kleeman, L. K., Jiang, H. H., Gordon, G., Goldman, J. E., Berry, G., Herman, B., and Levine, B. (1998) *J. Virol.* **72**, 8586–8596
11. Oberstein, A., Jeffrey, P. D., and Shi, Y. (2007) *J. Biol. Chem.* **282**, 13123–13132
12. Maiuri, M. C., Le Toumelin, G., Criollo, A., Rain, J. C., Gautier, F., Juin, P., Tasdemir, E., Pierron, G., Troulinaki, K., Tavernarakis, N., Hickman, J. A., Geneste, O., and Kroemer, G. (2007) *EMBO J.* **26**, 2527–2539
13. Liang, C., Feng, P., Ku, B., Dotan, I., Canaani, D., Oh, B. H., and Jung, J. U. (2006) *Nat. Cell Biol.* **8**, 688–699
14. Pattingre, S., Tassa, A., Qu, X., Garuti, R., Liang, X. H., Mizushima, N., Packer, M., Schneider, M. D., and Levine, B. (2005) *Cell* **122**, 927–939
15. Schuck, P. (2000) *Biophys. J.* **78**, 1606–1619
16. Nguyen, A. W., and Daugherty, P. S. (2005) *Nat. Biotechnol.* **23**, 355–360
17. Manser, E., Huang, H. Y., Loo, T. H., Chen, X. Q., Dong, J. M., Leung, T., and Lim, L. (1997) *Mol. Cell. Biol.* **17**, 1129–1143
18. Furuya, N., Yu, J., Byfield, M., Pattingre, S., and Levine, B. (2005) *Autophagy* **1**, 46–52
19. Thuduppathy, G. R., and Hill, R. B. (2006) *Protein Sci.* **15**, 248–257
20. Huang, Q., Petros, A. M., Virgin, H. W., Fesik, S. W., and Olejniczak, E. T. (2002) *Proc. Natl. Acad. Sci. U. S. A.* **99**, 3428–3433
21. Liang, X. H., Yu, J., Brown, K., and Levine, B. (2001) *Cancer Res.* **61**, 3443–3449
22. Denisov, A. Y., Sprules, T., Fraser, J., Kozlov, G., and Gehring, K. (2007) *Biochemistry* **46**, 734–740
23. O'Neill, J. W., Manion, M. K., Maguire, B., and Hockenbery, D. M. (2006) *J. Mol. Biol.* **356**, 367–381
24. Feng, W., Huang, S., Wu, H., and Zhang, M. (2007) *J. Mol. Biol.* **372**, 223–235
25. Ionov, Y., Nowak, N., Perucho, M., Markowitz, S., and Cowell, J. K. (2004) *Oncogene* **23**, 639–645
26. Bouillet, P., Cory, S., Zhang, L. C., Strasser, A., and Adams, J. M. (2001) *Dev. Cell* **1**, 645–653